第 35 卷第 8 期 无 机 化 学 学 报 Vol.35 No.8
2019 年 8 月 CHINESE JOURNAL OF INORGANIC CHEMISTRY 1427-1435

# 浸渍法制备钾基半焦在烟气脱硫中的循环再生

吴海涛[1,2] 卓启东[2] 杨 子[1,2] 石建东[2] 程洪见[2]
殷文宇[2] 唐晓艳[2] 马运声*[,2] 袁荣鑫*[,2]
([1]苏州大学化学化工与材料科学学院,苏州 215500)
([2]常熟理工学院,江苏省新型功能材料重点实验室,常熟 215500)

**摘要**: 采用碳酸钾($K_2CO_3$)与活化半焦通过浸渍法制备用于除去烟气 $SO_2$ 的催化脱硫材料(K/ASC)。研究表明,将活化半焦(ASC)通过 10%(质量分数)$K_2CO_3$ 改性获得钾基半焦(K10),其在 120 ℃时具有良好的 $SO_2$ 脱除效率,而且随着再生温度的升高(400~700 ℃),再生后 K10 的脱硫活性明显提高。K10(K10-R-600-*n*)的循环再生测试表明,样品在 4 次再生循环(K10-R-600-4)后具有最佳的脱硫性能,其硫容量为 68.9 mg·g$^{-1}$,比 K10(55.4 mg·g$^{-1}$)高 24.37%。再生分析脱硫产物为物理吸附的 $SO_2$,$H_2SO_4$ 和硫酸盐,再生后未分解的硫酸盐沉积会降低样品的脱硫活性。经过 10 次循环再生(K10-R-600-10),样品的硫容量为初始钾基半焦 K10 的 70%。

**关键词**: 半焦; $SO_2$; 脱硫; 循环再生
**中图分类号**: O643.3; TF704.3 **文献标识码**: A **文章编号**: 1001-4861(2019)08-1427-09
**DOI**:10.11862/CJIC.2019.175

# Cyclic Regeneration of Potassium-Modified Activated Semi-coke by Impregnation Method for Flue Gas Desulfurization

WU Hai-Tao[1,2] ZHUO Qi-Dong[2] YANG Zi[1,2] SHI Jian-Dong[2] CHEN Hong-Jian[2]
YIN Wen-Yu[2] TANG Xiao-Yan[2] MA Yun-Shen*[,2] YUAN Rong-Xin*[,2]
([1]*College of Chemistry, Chemical Engineering and Materials Science of Soochow University, Suzhou, Jiangsu* 215500, *China*)
([2]*Key Laboratory of Advanced Functional Materials, Changshu Institute of Technology, Changshu, Jiangsu* 215500, *China*)

**Abstract:** The potassium modified Activated Semi-coke (K/ASC) for $SO_2$ removal was prepared using potassium carbonate ($K_2CO_3$) by the impregnation method. The ASC modified by 10%(*w*/*w*) $K_2CO_3$ (K10) exhibited good $SO_2$ removal efficiency at 120 ℃. From 400 to 700 ℃, the higher the regeneration temperature is, the better is the desulfurization activity of K10 after regeneration. Cyclic regeneration of K10 (K10-R-600-*n*) showed that the sample had the best desulfurization performance after four regeneration cycles (K10-R-600-4), and its sulfur capacity was 68.9 mg·g$^{-1}$, 24.37% higher than that of K10 (55.4 mg·g$^{-1}$). The desulfurization products are divided into physisorbed $SO_2$, $H_2SO_4$ and sulfate. The deposition of sulfate, which does not decompose after regeneration, results in the decrease of the desulfurization activity. The sulfur capacity of the sample after ten regeneration cycles (K10-R-600-10) remained 70% that of the fresh K10.

**Keywords:** semi-coke; $SO_2$; desulfurization; cyclic regeneration

收稿日期:2018-11-22。收修改稿日期:2019-05-30。
国家自然科学基金(No.21201068,21201025)和江苏省自然科学基金(No.2016050)资助项目。
*通信联系人。E-mail:yuanrx@cslg.edu.cn

## 0 Introduction

Sulfur dioxide ($SO_2$) is one of the major air pollutants that can cause various problems to the environment and public health. The thermal power and steel industries are leading sources for the emission of $SO_2$[1]. In order to solve the problem of $SO_2$ pollution, many technologies have been developed. Among these, the adsorption-catalysis technology for $SO_2$ removal of flue gas has a good prospect of application[2-4].

Many studies have indicated that carbonaceous materials, including activated carbon, coke, semi-coke, and activated carbon fibers, can effectively remove $SO_2$ with little negative effect on the environment. The carbonaceous materials have excellent performance in the absorption of $SO_2$ due to high surface area, rich pore structure and oxygen-containing functional groups on the carbon surface[5-6]. Previous studies have shown that activated carbon (coke) modified by metal or their oxides, such as Fe[7-8], V[9], Ti[10] and Mn[11], can significantly improve the desulfurization capacity, but with the process of reaction, the desulfurization capacity would decline due to the deposition of desulfurization byproducts on the surface or in the pore of catalysts. The study by Guo[12] has shown that Fe modified activated carbon has a sulfur capacity of 231 $mg \cdot g^{-1}$, using $Fe_2O_3$, $Fe_3O_4$ and FeO as the active components, but the generated sulfate in the desulfurization process, such as $Fe_2(SO_4)_3$, can result in a loss of active components. The adsorbate in the pore or on the surface of catalysts can be removed by thermal regeneration. The regeneration temperatures could not be too high for industrial applications. As reported by Liu et al.[3], the iron-modified activated coke that has $SO_2$ removal activity at 200 ℃ was regenerated in $NH_3$ at 350 ℃. Guo et al.[13] studied the desulfurization activity of Ni/AC and the result shows that the catalyst calcined at 550 ℃ and 800 ℃ has a higher desulfurization activity. The study by Li et al.[14] has shown that CuO/AC catalyst lodaed with 1%(*w*/*w*) $CeO_2$ possesses the best desulfurization effect. $CeO_2$ additive enhances the dispersion degree of CuO on the surface of the catalyst.

In this study, the potassium-modified activated semi-coke (K/ASC) prepared by impregnation method, which shows high $SO_2$ removal ability at 120 ℃, was used to investigate its regeneration properties for flue gas desulfurization. The desulfurization performance and surface chemistry of the regenerated K/ASC were carefully analyzed via X-ray photoelectron spectroscopy (XPS), scanning electron microscope (SEM), X-ray powder diffraction (XRD), *etc*. In addition, the regeneration mechanism of the ASC modified by metal was discussed.

## 1 Experimental

### 1.1 Preparation of catalyst

All chemicals used in this work were analytic reagent grade. The original semi-coke was first crushed and sieved to 10~20 mesh (referred to as SC). The SC particles were activated using nitric acid (10%, *w*/*w*) at 200 ℃ for 2 h in a stainless steel autoclave, and the particles were washed with distilled water until pH=7.0 in the washing liquid after activating, then dried at 120 ℃ for 8 h (referred to as ASC).

Catalysts were prepared by impregnation. Potassium carbonate was dissolved in distilled water as the precursors. 20 g of ASC was impregnated with 20 mL of the precursor to achieve 2.5%, 5%, 7.5%, 10% and 15%(*w*/*w*) $K_2CO_3$ loading, and dried at 120 ℃ in an oven overnight. The samples were calcined in a tube furnace from room temperature to 600 ℃ with a heating rate of 5 $℃ \cdot min^{-1}$ under $N_2$ and maintained for 2 h, then cooled to room temperature in $N_2$, labeled as K2.5, K5, K7.5, K10, K15, respectively.

### 1.2 Desulfurization and regeneration

The desulfurization activity of samples was evaluated in a fixed-bed reactor under atmospheric pressure, and the experimental apparatus is presented in Fig.1.

A sample (20 g) was packed into the reactor. The simulated flue gas contained 0.09%(*V*/*V*) $SO_2$, 11%(*V*/*V*) $O_2$, and $N_2$ as balance. The gas flow velocity was 900 $mL \cdot min^{-1}$. The inlet and outlet concentration of $SO_2$ were monitored online by a flue gas analyzer continuously, and the desulfurization test was stopped

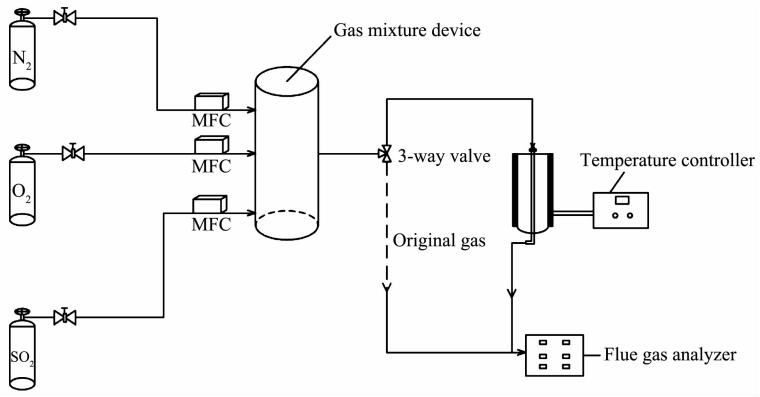


Fig.1　Flowchart of the experimental system

when the outlet concentration of $SO_2$ reached 10% of the inlet. The sulfur capacity was determined by the integration of the $SO_2$ breakthrough curve and was presented as the amount of $SO_2$ removal per unit mass of activated semi-coke, while the corresponding working time was regarded as the breakthrough time. The sulfur capacity of samples were calculated based on the following formula[15]:

$$Sc=\int_0^t \frac{MQ(C_0-C_t)10^{-6}}{22.4m}dt$$

where Sc is sulfur capacity ($mg\cdot g^{-1}$), $M$ the $SO_2$ molecular weight, $Q$ the gas flow ($mL\cdot min^{-1}$), $t$ the working time, $C_0$ the inlet $SO_2$ concentration, $C_t$ the outlet $SO_2$ concentration at working time of $t$, and $m$ the sample mass.

The used K10 (referred to as K10-S) was regenerated in a tube furnace at 400, 500, 600 and 700 ℃ for 2 h in a pure $N_2$ (Flow rate: 50 $mL\cdot min^{-1}$). The heating rate was 5 $℃\cdot min^{-1}$. Then the sample was cooled to room temperature in $N_2$ atmosphere. The thermal-regenerated sample was denoted as K10-R-$T$, where $T$ is the regeneration temperature.

### 1.3　Characterization of catalyst

X-ray photoelectron spectroscopy (XPS) was applied to determine the surface chemical composition and functional groups, using an XSAM-800 spectrometer (KRATOS Co., UK) with Al (1 486.6 eV) under ultrahigh vacuum (UHV) at 12 kV and 15 mA. Scanning electron microscopy (SEM) was used to obtain the surface morphology of the samples. It was taken in Sigma scanning electron microscope (Carl Zeiss AG, Germany) with a voltage of 20 kV. X-ray powder diffraction (XRD) was performed in a multifunctional X-ray diffractometer using Cu $K\alpha$ radiation ($\lambda$=0.154 06 nm) at a rate of $10°\cdot min^{-1}$ from 5° to 90° ($2\theta$) and operated at 30 kV and 30 mA. The structure parameters of the samples were measured at −196 ℃ using ASAP 2020 analyzer. The specific surface areas ($S_{BET}$) was calculated using the BET equation by $N_2$ adsorption. The micropore volume ($V_{micro}$) was calculated by a t-plot method. The Fourier transform infrared spectroscopy (FTIR) spectra were recorded using the KBr pellet technique on a Thermo spectrometer in the 4 000~400 $cm^{-1}$ spectral range.

## 2　Results and discussion

### 2.1　Desulfurization activity test

The relationship between outlet concentration of $SO_2$ and working time of all samples is presented in Fig.2. The corresponding sulfur capacity and breakthrough time are summarized in Table 1.

ASC exhibited better $SO_2$ removal ability

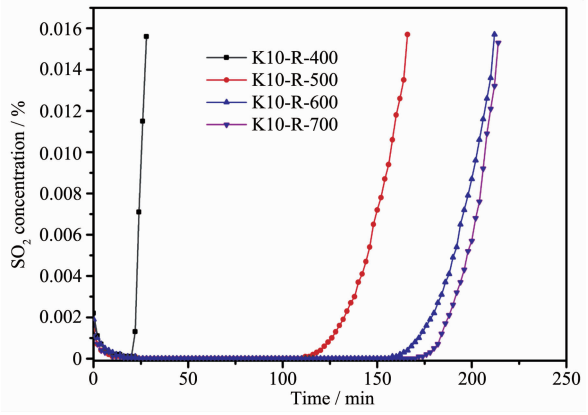


Fig.2　Relationship between outlet concentration of $SO_2$ and working time at 120 ℃

**Table 1 Breakthrough sulfur capacity and breakthrough time of the catalysts at 120 ℃**

| Sample | Sulfur capacity / (mg·g$^{-1}$) | Breakthrough time / min |
|---|---|---|
| SC | 1.5 | 5 |
| ASC | 23.8 | 102 |
| K2.5 | 28.5 | 124 |
| K5 | 35.3 | 136 |
| K7.5 | 40.9 | 162 |
| K10 | 55.4 | 188 |
| K15 | 56.2 | 190 |

compared to SC, showing that nitric acid pretreatment can improve the $SO_2$ removal ability. This might be due to an increase of oxygen containing functional groups on the surface of activated semi-coke after nitric acid treatment[13]. The sulfur capacity of K/ASC samples was significantly improved when $K_2CO_3$ species were blended into activated semi-coke, indicating that $K_2CO_3$ species plays a key role in the $SO_2$ removal process. As the ratio of $K_2CO_3$ on activated semi-coke was increased from 2.5% to 15%, the sulfur capacity and breakthrough time increased gradually. K15 exhibited the best $SO_2$ removal ability with the breakthrough sulfur capacity of 56.2 mg·g$^{-1}$ and the breakthrough time of 190 min. The $SO_2$ removal ability of K10 was similar to K15 and corresponded to breakthrough sulfur capacity of 55.4 mg·g$^{-1}$ and breakthrough time of 188 min, which means that when the ratio of $K_2CO_3$ was higher than 10%, the desulfurization capacity was not obviously increased. In Fig.2, it shows that the desulfurization activity of K10 is improved significantly with increasing of the regeneration temperature from 400 to 600 ℃. However, the breakthrough time of K10 basically unchanged when the regeneration temperature exceeded 600 ℃. According to the results in Table 1 and Fig.2, the $SO_2$ removal ability of the samples is in the order: AC<ASC<K2.5<K5<K7.5<K15≈K10, and K10-R-400<K10-R-500<K10-R-700≈K10-R-600.

In order to study their regeneration performance, K10 was selected for thermal regeneration test. The samples after regeneration were denoted as K10-R-600-*n*, where *n* is the number of regeneration cycle. The desulfurization performance of K10-R-600-*n* expressed as sulfur capacity and breakthrough time is shown in Table 2.

As shown above, the desulfurization performance of the K10-R-600-*n* can be divided into two stages: one is the increasing stage from the 1st to the 4th regeneration cycle; the other is the decreasing stage from the 5th to the 11th regeneration cycle respectively.

**Table 2 Sulfur capacity and breakthrough time of the regenerated K10**

| Sample | Sulfur capacity / (mg·g$^{-1}$) | Breakthrough time / min |
|---|---|---|
| K10 | 55.4 | 188 |
| K10-600-1 | 56.0 | 190 |
| K10-600-2 | 62.5 | 212 |
| K10-600-3 | 66.6 | 226 |
| K10-600-4 | 68.9 | 242 |
| K10-600-5 | 61.3 | 208 |
| K10-600-6 | 52.5 | 178 |
| K10-600-7 | 51.9 | 176 |
| K10-600-8 | 48.3 | 164 |
| K10-600-9 | 47.2 | 160 |
| K10-600-10 | 38.9 | 132 |
| K10-600-11 | 36.6 | 124 |

In the increasing stage, the desulfurization performance of K10-R-600-*n* showed a certain degree of improvement with increasing regeneration cycles. The regeneration treatment can significantly increase the oxygen functional groups on surface of K10, especially the basic functional groups, which contributed more to the desulfurization performance[15]. The sulfur capacity reached its maximum after four regeneration cycles, the sulfur capacity of K10-R-600-4 was 68.9 mg·g$^{-1}$, 24.37% much higher than that of K10. From the fifth regeneration cycle, the desulfurization activity of K10-R-600-*n* entered declining phase and lower than that of K10, except K10-R-600-5. The reduction of desulfurization performance became slow from the sixth to the ninth regeneration cycle. The sulfur capacity of K10-R-600-9 was 47.2 mg·g$^{-1}$, which was 85.20% of K10. K10-R-600-10 showed a clear reduction of the sulfur capacity, which decreased from 47.2 to 38.9 mg·g$^{-1}$ and was 70.22% of K10. Jiang et al.[16] studied cyclic regeneration of pyrolusite-modified activated coke (ACP) for flue gas desulfurization, and the results showed that the sulfur capacity was less than 50% of the ACP after ten regeneration cycles. In this study, the desulfurization performance of K10 increases from the first to the fourth regeneration cycle and maintains relatively better desulfurization capacity even after ten regeneration cycles. It is worth noting that the catalyst is a high-activity and low-cost SC desulfurizer, and has industrial application prospects.

## 2.2　Study of surface species after $SO_2$ removal

In order to study the changes of surface species after $SO_2$ removal, K10 and K10-S were characterized by XPS, XRD, $N_2$ adsorption-desorption, FTIR and SEM. In Fig.3 (XPS spectra), the S2*p* spectra of the catalysts before and after desulfurization are fitting into two peaks. $S^{6+}$ binding energy of K10 and K10-S were 168.78 and 169.71 eV, respectively, and they correspond to $SO_4^{2-}$[17-18]. It is proved that $SO_4^{2-}$ is derived from the oxidation reaction of $SO_2$ and $O_2$ on the surface of catalysts. $S^0$ binding energy of K10 and K10-S were 164.31 and 164.34 eV[19-20], respectively, which correspond to original species of catalysts. This

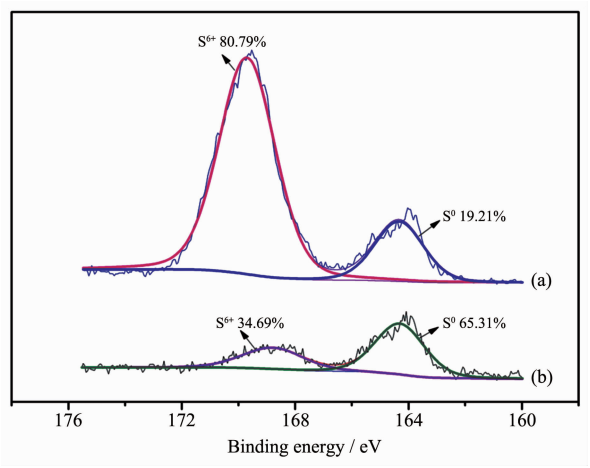


Fig.3　XPS spectra of S2*p* for K10-S (a) and K10 (b)

result shows that the absorbed $SO_2$ is basically oxidized to $SO_4^{2-}$.

In Fig.4(a), the diffraction peaks observed at 2$\theta$= 31.03°, 38.78°, 49.21° and 57.56° are attributed to $K_2CO_3$ (PDF No.27-1348). In Fig.4(b), some peaks of K10-S disappear or change compared to that of K10. The diffraction peaks of $K_2SO_4$ at 2$\theta$=29.75°, 30.78°, 40.42°, 43.02°, 43.28°, 43.43°, 53.51°, 58.70° (PDF No.05-0613) were observed. It means that $K_2CO_3$ is transformed into $K_2SO_4$ after desulfurization. As shown in Fig.5, the intensity of $K_2CO_3$ is recovered relatively after regenerating. In Fig.5(b), the peaks belonging to $K_2SO_4$ become more intense comparing to that in Fig.5 (a). This means that $K_2SO_4$ would accumulate gradually in the K10 with an increase of desulfurization-regeneration cycles.

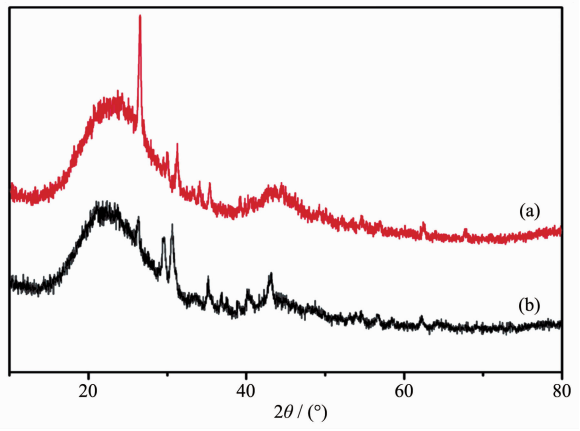


Fig.4　XRD patterns of K10 (a) and K10-S (b)

The structure parameters listed in Table 3 show that the $S_{BET}$ linearly increased as the regeneration

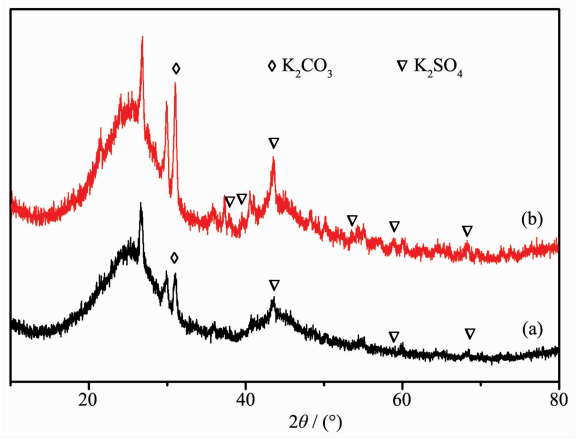


Fig.5 XRD patterns of K10-600-1 (a) and K10-600-5 (b)

cycle increased. The change reveals that the regeneration of K10 acts as a further activation, which improve the pore structure of catalyst effectively. The $V_{micro}$ changed irregularly after seven regeneration cycles, because the excessive activation could cause the collapse of the adjacent wall structures between the micropores. Similar observations have also been reported by Yang et al[15,21]. The desulfurization performance of the K10-600-*n* gradually decreased after the forth regeneration cycle. It means that the structure parameters are not the key factor for the desulfurization of K10. In Table 4, the mass loss rate linearly decreases as the regeneration cycle increases, showing that the carbon has been partially consumed during the regeneration process.

As shown in Fig.6 (IR spectra), the bands at 3 441 and 3 131 $cm^{-1}$ correspond to the -OH stretching vibration. The bands at 1 627 and 1 400 $cm^{-1}$ can be identified as the anti-symmetrical and symmetrical vibrations of carbonyl groups. After desulfurization, for K10-S, some new bands were detected at 1 127 and 524 $cm^{-1}$ (Fig.6b), which are assigned to the S-O or S =O stretching mode adsorbed sulfate ions and sulfate, showing the formation of $H_2SO_4$ and $K_2SO_4$.

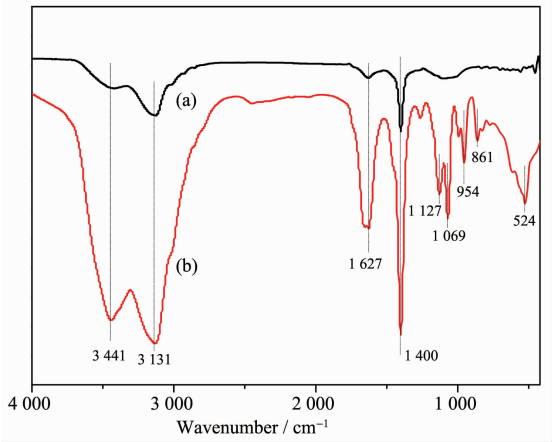


Fig.6 FTIR spectra of K10 (a) and K10-S (b)

**Table 3 Structure parameters calculated from nitrogen adsorption isotherms**

| Sample | $S_{BET}$ / ($m^2 \cdot g^{-1}$) | $V_{micro}$ / ($cm^3 \cdot g^{-1}$) |
|---|---|---|
| ASC | 70 | 0.028 |
| K10 | 167 | 0.062 |
| K10-600-1 | 173 | 0.066 |
| K10-600-2 | 178 | 0.069 |
| K10-600-3 | 182 | 0.073 |
| K10-600-4 | 190 | 0.075 |
| K10-600-5 | 207 | 0.083 |
| K10-600-6 | 213 | 0.087 |
| K10-600-7 | 218 | 0.091 |
| K10-600-8 | 221 | 0.086 |
| K10-600-9 | 229 | 0.083 |
| K10-600-10 | 237 | 0.084 |
| K10-600-11 | 241 | 0.078 |

**Table 4 Mass loss rate of the sample after regeneration**

| Sample | K10-600-4 | K10-600-6 | K10-600-8 | K10-600-10 |
|---|---|---|---|---|
| Mass loss rate / % | 2.74 | 4.94 | 7.32 | 9.58 |
| $S_{BET}$ / ($m^2 \cdot g^{-1}$) | 190 | 213 | 221 | 237 |

The C-O stretching at 1 069 $cm^{-1}$ of carbonyl groups in alcohols, ethers, or phenols and the out-of-plane bending vibration of C-H groups in aromatic at 861 $cm^{-1}$ and in olefin at 954 $cm^{-1}$ were observed. These results indicate that the surface functional groups are constantly updated in desulfurization process[12,22].

SEM images of the samples and element mapping image of K are shown in Fig.7. A large number of pores, cracks and few impurities were presented on the surface of K10 (Fig.7a). The spheroidal particles were also presented on the surface of K10 after desulfurization (Fig.7b) and a few of them would remain on the surface of K10 after regeneration (Fig. 7c). It can be better illustrated that the sulfate is deposited in pore or on the surface of the samples before and after regeneration. The mapping result shows potassium is evenly distributed on the semi-coke surface (Fig.7d).

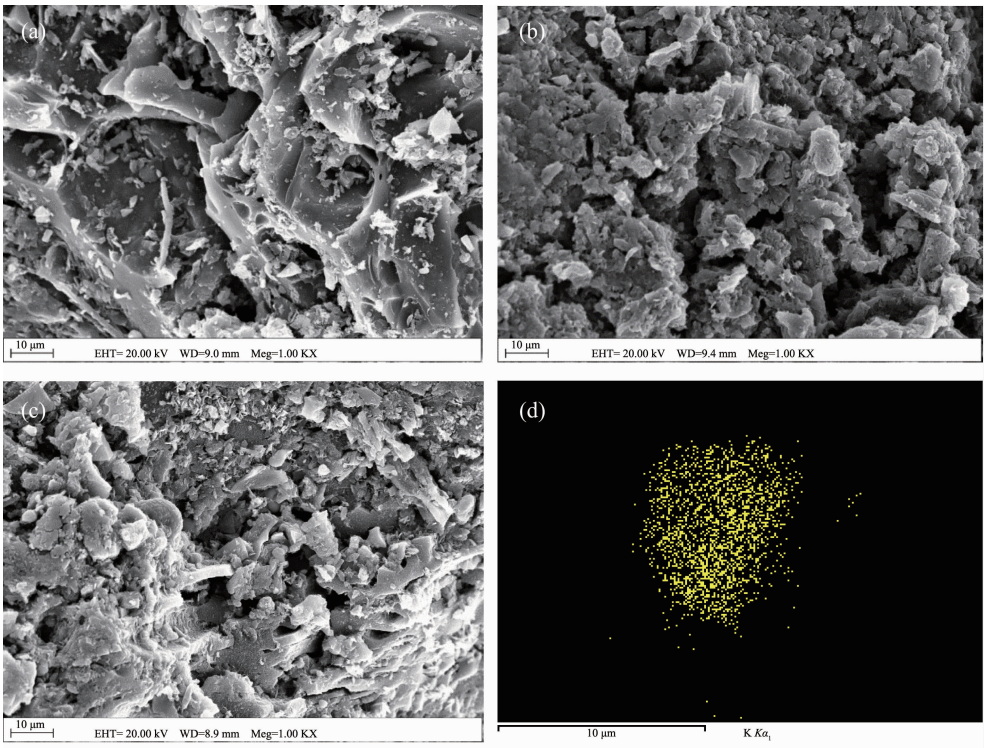


Fig.7　SEM images of the samples: K10 (a), K10-S (b), K10-R-600-1 (c), and element mapping image of K (d)

## 2.3　Regeneration mechanism

Fig.8 shows the outlet gas components of K10-S during the regeneration process. The regeneration process of K10-S could be divided into three stages: at the first stage, the temperature was lower than 170 ℃; the second stage was in the temperature range of 170 ~490 ℃; the temperature from 490 ℃ to the isothermal stage was the last stage. For the metal-modified AC, there are three kinds of sulfur species (*i.e.*, adsorbed $SO_2$, sulfur acid, and metal sulfate) coexisting in the pore structure after desulfurization[3,23-24]. During the regeneration process, the adsorbed $SO_2$ could be desorbed easily when the temperature reached 150 ℃, and this stage is called desorption. When the temperature was increased to 200 ℃, the sulfur acid could react with the carbon to release $SO_2$,

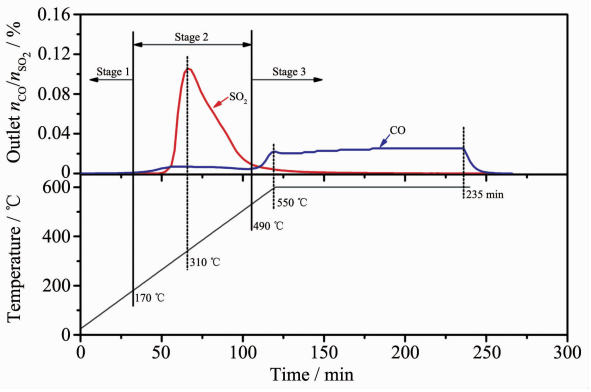


Fig.8　Outlet gas components of K10-S during regeneration progress

which is called reaction[25]. With the temperature was further increased, the sulfur acid was completely removed and the metal sulfate began to decompose when the temperature was high enough, which is called decomposition.

At the first stage, there was no CO, or $SO_2$ detected even though the temperature was increased to 170 ℃. This result indicates the amount of adsorbed $SO_2$ is very low on the surface of K10. In the second stage, the outlet concentration of $SO_2$ began to increase profoundly then gradually decreased. The outlet concentration of $SO_2$ reached the maximum value at 310 ℃. However, the concentration of CO increased gradually at first and then remained basically unchanged. In the third stage, the concentration of $SO_2$ was very low and gradually reduced with the increasing of temperature. It could be due to the residuals of $SO_2$ in the previous stage. It worth noting that the CO showed the second increase and reached the new vertex at 550 ℃, then remained basically stable and decreased rapidly before cooling. A slight increase of the CO in the third stage may be contributed to the pyrolysis and gasification of oxygen-containing functional groups in the presence of metals on the carbon matrix, which serve as further surface modification[15].

On the basis of the experimental results above, all of the potential reactions are as follows:

$$SO_2(ads) \longrightarrow SO_2(g) \quad (1)$$

$$C+H_2SO_4 \longrightarrow CO(g)+SO_2(g)+H_2O(g) \quad (2)$$

$$C+K_2SO_4 \longrightarrow K\text{-}X+S+CO(g)$$

(K-X: active K species) (3)

$$C\text{-}(CO) \longrightarrow CO(g) \quad (4)$$

$$C+SO_2 \longrightarrow S+CO(g) \quad (5)$$

## 3 Conclusions

The results show that activated semi-coke (ASC) modified by $K_2CO_3$ have higher desulfurization activity than ASC at 120 ℃ for $SO_2$ removal. ASC modified by different ratios of $K_2CO_3$ exhibits different $SO_2$ removal ability. $SO_2$ removal ability of the catalysts ranks as follows: K2.5 <K5 <K7.5 <K15 ≈K10. The used K10 can be fully regenerated in $N_2$ at 600 ℃. Cyclic regeneration of K10 shows that the K10 is a good desulfurizer, since its regeneration efficiency begins to increase and then decrease. After four regeneration cycles, the sample (K10-R-600-4) has the highest sulfur capacity (68.9 $mg \cdot g^{-1}$), which is 24.37% higher than that of K10 (55.4 $mg \cdot g^{-1}$). The desulfurization products are divided into physisorbed $SO_2$, $H_2SO_4$ and sulfate. Some sulfate could not be decomposed, which deposited in a pore or on the surface of the samples after regeneration. The outlet gas analysis of K10-S during the regeneration process shows that there is a reaction between carbon and $H_2SO_4$ or sulfate as the regeneration temperature increases. The deposition of sulfate leads to the decrease in the sulfur capacity of catalyst after five regeneration cycles. However, the desulfurization activity of catalyst remains relatively stable upon further reuse. Based on the high efficient of regeneration cycles, the catalyst can be used to absorb $SO_2$ from flue gas. The work opens up possibilities for using K/ASC as a promising agent for flue-gas desulfurization catalysis.

## References:


[1] Cui X X, Yi H H, Tang X L, et al. *J. Chem. Technol. Biotechnol.*, **2018**,**93**(3):720-729

[2] Mathieu, Y, Tzanis, L, Soulard, M, et al. *Fuel Process. Technol.*, **2013**,**114**(3):81-100

[3] Ma J, Liu Z, Liu S, et al. *Appl. Catal. B*, **2003**,**45**(4):301-309

[4] Jastrzb K. *Fuel Process. Technol.*, **2012**,**104**:371-377

[5] Liu Q Y, Li C H, Li Y X. *Carbon*, **2003**,**41**(12):2217-2223

[6] Liu X L, Guo J X, Chu Y H, et al. *Fuel*, **2014**,**123**(1):93100

[7] Gao X, Liu S, Zhang Y, et al. *J. Hazard. Mater.*, **2011**,**188**(1/2/3):58-66

[8] Davini P. *Carbon*, **2001**,**39**(3):419-424

[9] Guo Y, Liu Z, Liu Q, et al. *Catal. Today*, **2008**,**131**(1/2/3/4):322-329

[10]Zhang C, Yang D, Jiang X, et al. *Environ. Technol.*, **2016**, **37**(15):1895-1905

[11]Yang L, Jiang X, Yang Z S, et al. *Ind. Eng. Chem. Res.*, **2015**,**54**(5):1689-1696

[12]Guo J X, Luo H D, Shu S, et al. *Energy Fuels*, **2018**,**32**(1):765-776

[13]Guo J X, Liang J, Chu Y H, et al. *Chin. J. Catal.*, **2010**,**31**(3):278-282

[14]DOU Guang-Xiong(窦冠雄), LONG Yue(龙跃), ZHANG Liang-Jin(张良进), et al. *Iron Steel*(钢铁), **2018**,**853**(6):26-30

[15]Yang L, Jiang X, Jiang W J. *Energy Fuels*, **2017**,**31**(4):4556-4564

[16]Rodriguez-Reinoso F. *Carbon*, **1998**,**36**(3):159-175

[17]Qu Y, Guo J, Chu Y, et al. *Appl. Surf. Sci.*, **2013**,**282**(5):425-431

[18]Smirnov M Y, Kalinkin A V, Pashis A V, et al. *Kinet. Catal.*, **2003**,**44**(4):575582

[19]Liu F D, Asakur K, He H, et al. *Appl. Catal. B*, **2011**,**103**(3/4):369-377

[20]Liu L, Liao L H, Meng Q H, et al. *Carbon*, **2015**,**90**:75-84

[21]Jung S, Oh S, Choi G, et al. *J. Anal. Appl. Pyrolysis*, **2014**, **109**:123-131

[22]Zhao L, Li X Y, Hao C, et al. *Appl. Catal. B*, **2012**,**117-118**:339-345

[23]Collins J, Zheng D, Ngo T, et al. *Carbon*, **2014**,**79**:500-517

[24]Gao X, Liu S, Zhang Y, et al. *J. Hazard. Mater.*, **2011**,**188**(1/2/3):58-66

[25]Yan Z, Liu L L, Zhang Y L, et al. *Energy Fuels*, **2013**,**27**(6):3080-3089